Journal homepage www.jzs.univsul.edu.iq
Journal of Zankoy Sulaimani
Part-A- (Pure and Applied Sciences)
ISSN:1812-4100

Structural and Optical Properties of R6G Doped Nanotitania Thin Films Deposited via Sol–Gel Dip-coating Method

Muhammad A. Saeed[1], Majida A. Ameen [1]& Aras S. Mahmood [1]

[1] *Department of Physics, College of Education, University of Sulaimani, Sulaimani, Kurdistan Region, Iraq*
**Corresponding author's E-mail: muhammad.saeed@univsul.edu.iq*

Article info

Original: 08 /7/ 2021
Revised: 25/10/2021
Accepted: 25/10/2021
Published online: 20/6/2022

Key Words:
Nanostructure TiO_2 thin films, R6G dye, dip-coated sol-gel, fluorescence emission spectrum.

Abstract

Pure and rhodamine 6G (R6G) doped titanium dioxide (TiO_2) nanostructure thin films with different concentrations (3×10^{-4}, 3×10^{-5}, 3×10^{-6}, and 3×10^{-7}) M of doped TiO_2 sol were deposited on glass substrate via dip-coated sol-gel method. Amorphous structure of the pure and doped TiO_2 thin films was identified by X-ray diffraction (XRD) technique. UV-Visible (UV-vis) and fluorescence spectrophotometry techniques were used to study optical and spectroscopic characterization of the samples, respectively. The absorption spectra for all pure and doped TiO_2 films indicate a strong absorbance in the UV region which open the possible application of these films for UV filter optical element. 50 nm blue shift of the absorption edge for the TiO_2 films with respect to the sol was observed which proves the nanostructure texture of TiO_2 thin films. Upon increasing dye concentration, a red shift in the maximum fluorescence emission peaks of R6G ethanolic solution and doped TiO_2 sol was observed. The presence of R6G dye molecules in the matrix of TiO_2 films is demonstrated by the appearance of two distinct intensity fluorescence peaks at 540 and 600 nm. Various fluorescence peaks of R6G doped TiO_2 thin films were observed in UV-vis region under 300 nm pumping wavelength.

Introduction

Nanostructured materials have attracted significant interest due to their unique electrical, optical, magnetic, chemical and mechanical properties, which cannot be accomplished by their bulk form [1].

Amongst different methods for nanomaterials preparation, low-temperature sol-gel process is one of the most common method for preparing amorphous and nanocrystalline metallic oxide material at a laboratory scale [2]. This method is also used to obtain and examine the concentration-dependent fluorescence properties of organic dye and inorganic materials trapped in oxide materials [3, 4].

Generally, in a conventional sol-gel method, the hydrolysis and polymerization processes of the precursors produce a colloidal suspension or sol, which transitions from the liquid sol to the solid gel phase upon complete polymerization and lack of solvent. With more drying and hydrothermal treatment, the wet gel can be converted into nanocrystals [5].

Furthermore, the sol–gel method is a promising procedure with considerable advantages, including better mixing at the molecular level of the raw materials and superior chemical homogeneity of the final product [6]. Despite of its advantages, sol-gel processing has some limitations including; long processing times health hazard of some organic solutions, large shrinkage [7]. Deposition of thin films on glass, ceramics, metal, semiconductor and plastic substrates is one of the most important applications of the sol-gel method [2, 7].

Single and multi-component oxide coatings can be achieved by spray, spin or dip-coating on a wide scale at a lower cost than other methods [8].
The sol–gel process allows the synthesis of optical materials through the fabrication of a transparent host, offering for the addition of high dopant concentrations to the optical materials [9].
One of the best candidate material, which has attracted considerable interest is pure and doped TiO_2 [3, 10]. Due to its high transparency in the visible and infrared regions, TiO_2 absorbs in the ultraviolet region [11], it has a high refractive index, wide band gap, and high chemical stability [12], photostability [13], thermal stability and strength [14]. It is also non-toxic, inexpensive, highly photoactive, and easily synthesized and handled [15].
TiO_2 also considered to be a prospective host for organic guests [16]. In addition, TiO_2 has been used in a variety of fields, including photovoltaic solar cells, gas sensors [17], photocatalysts [12], integrated electronics, anti-reflect coating [18], protective coatings, and optical components [19].
The incorporation of organic molecules within an inorganic network can improve the matrices' properties. Organic compounds can contribute to a unique property (optical or electrical properties, electrochemical reactions, chemical or biochemical reactivity). The inorganic component, on the other hand, contributes to the its mechanical and thermal strength, allowing it to modulate the optical index and developing desirable electrochemical, electrical, and magnetic properties on its own [16].
A variety of laser dyes have been incorporated in various sol-gel matrices, and tunable laser action has been demonstrated with these materials [20]. Xanthene dyes are among the most widely used laser dyes [21]. R6G is a xanthene derivative that is commonly employed in dye lasers as a gain medium. R6G has been shown to be able to be incorporated into sol-gel matrices such as nanostructure TiO_2 [10, 17, 21].
Because of its high absorption and emission cross-sections ($4x10^{-16}$ cm^2) and photo-stability, rhodamine 6G dye (R6G) is the material of choice for many applications and demonstrations [22]. R6G is a cationic dye with a strong visible absorption and a high fluorescence yield. The molecule consists of two chromophores, a dibenzopyrene chromophore (xanthene) and a carboxyphenyl group tilted by approximately 90^o with respect to the xanthene [23]. In order to determine the rate and direction of flow and transport, R6G is often employed as a tracer dye in water. Fluorescence microscopy, flow cytometry, and fluorescence correlation spectroscopy are some examples of R6G dye applications [24].
The intensive and wide survey of literature reveals that, although many studies have investigated R6G doped TiO_2 matrices [3, 10, 11, 17, 25, 26]. There are no studies in the literature examining the effect of R6G on the fluorescence emission peak of TiO_2 matrices. This suggests manufacturing the hybrid R6G-TiO_2 active medium laser and optoelectronic device.
In this work, the nanostructured R6G doped TiO_2 thin films with different concentrations of R6G dye (C_{R6G}) were prepared by dip-coated sol–gel method on a glass substrate. The structural and optical properties of these films were studied using XRD, UV–vis spectrophotometry and spectrofluorophotometery.

Experimental

A. Chemical materials

Titanium (IV) isopropoxide ($Ti[OC(CH_3)_2]_4$; TTIP) (≥ 97%) supplied by Sigma-Aldrich was used as a starting material. Ethanol (C_2H_5OH, 99.9%; EtOH) (CHEM-LAB) acted as the solvent and hydrochloric acid (HCl, 37%; Merck) acted as the catalyst. Deionized water was used to hydrolyze TTIP and prepare TiO_2 sol. R6G dye ($C_{28}H_{31}N_2O_3Cl$) (100%) supplied as a powder was used for doping TiO_2 thin films. All regents were used as received.

B. Samples preparation

Pure TiO_2 sol was prepared by mixing, at room temperature (RT), TTIP, deionized water, EtOH, and HCl in terms of a molar ratio of TTIP:H2O:EtOH: HCl = 1:1:10:0.1. The solution was left for 10 minutes under magnetic stirring. These procedures were carried out in a cooler water jacket at temperature (10˚C - 14˚C). The obtained sol was aged 24 hours before coating on microscope glass substrates; (76×26×1mm) supplied by SUPE-RIOR Germany. The substrate (25×10) mm^2 were first cleaned with detergent then rinsed with running water after that they were cleaned with distilled water and ethanol alcohol. The substrate was immersed in the TiO_2 sol and withdrawn at controlled speed of (0.7 $mm.s^{-1}$). Finally, the coated gel thin films were dried in an ambient atmosphere at RT (26-29 °C).

The R6G doped nanostructured TiO_2 thin films were synthesised with using the following steps: First, R6G was dissolved in EtOH to produce C_{R6G}= 1×10^{-2}, 1×10^{-3}, 1×10^{-4}, and 1×10^{-5} M solutions. Second, TTIP:R6G =1:0.1 (g/ml) was added into TTIP:H_2O:EtOH: HCl = 1:1:10:0.1 mixture that prepared by the same above procedure, to obtain R6G doped TiO_2 sols with 3×10^{-4}, 3×10^{-5}, 3×10^{-6}, and 3×10^{-7} M concentrations which was ready to be deposited on the glass substrate. Finally, the pure and doped TiO_2 coating thin films were characterized more than month after deposition.

C. Characterization of samples

To analyses the structural characteristics of the synthesized pure and doped TiO_2 thin films, XRD patterns were obtained using an x-ray diffractometer, Shimadzu, Japan, XRD-6000 instrument with CuKα radiation (λ = 1.54060 Å). Absorption spectra of the different concentration of R6G solution, pure and doped TiO_2 sols and thin films, were measured with a UV–vis spectrophotometer, Agilent Cary 60. Fluorescence emission spectra of these samples were measured using a fluorescence spectrophotometer, Agilent Carry Eclipse.

Results and Discussion

A. X-Ray Diffraction Analysis (XRD)

XRD measurements have been carried out, at RT. Figure: 1 shows XRD patterns for three kinds of samples; glass substrate (blank), pure, and R6G doped TiO_2 thin films with 3×10^{-4} and 3×10^{-7} M concentrations, deposited on glass substrate. There is no distinct diffraction peak, and only one broad scattering peak appears at nearly 25º belongs to the glass substrate, and can be interpreted as evidence of the presence of amorphous SiO_2 [27]. The XRD pattern are similar and confirmed that all (doped and undoped) TiO_2 matrices are primarily amorphous [16].

The XRD spectra did not show any evidence peak related to TiO_2 phase this is indicate a dominant substrate structure and amorphousity of films.

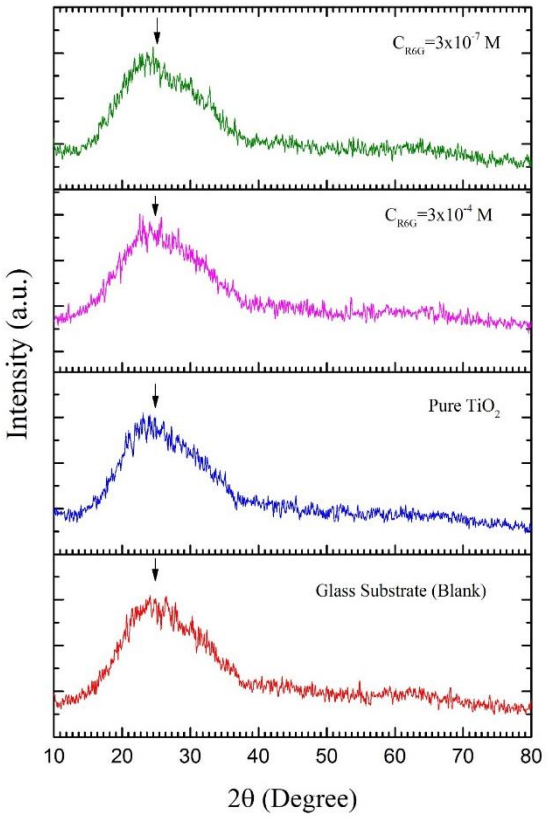

Figure-1: XRD patterns of glass substrate (blank), pure, 3×10^{-4} and 3×10^{-7} M R6G doped TiO_2 thin films, deposited on glass substrate.

B. Optical Characterization

Absorption Spectra

UV-vis Spectroscopy is one of most widely used techniques to determine the optical properties of various types of materials (solution, sol and solids) in different forms (colloids, nanoparticles, thin films and bulk materials). Firstly, the absorption spectrum of R6G ethanolic solution with different concentration from 1×10^{-2} - 1×10^{-5} M were measured at RT and tested using a quartz cell of one 1 cm optical path and presented in *Figure: 2* which reveals the variation of the spectra for different concentration. From this figure, it is clear that the high concentration 1×10^{-2} M; stock solution, exhibit a signal saturation. With decreasing concentration into 1×10^{-3} M, the absorption spectra exhibit the monomer and aggregates contributions which make a broad band spectrum in the range of (432-584) nm as well as a red shifted peak at 387 nm corresponding to the excited singlet state S_1. By diluting the concentration to 1×10^{-4} M the absorption spectrum of the solution is characterized by the superposition of two bands at around 490 and 530 nm as well as maxima at 347, 276, and 247 nm corresponding to the excited singlets S_2, S_3, and S_4 respectively.

For further lower concentration at 1×10^{-5} M the dye dissolves practically completely into monomer. The absorption spectrum is determined by the intrinsic absorption of the dye molecules and the dye-solvent interaction, whereas dye-dye interaction is negligible because of the large average distance between the dye molecules. This is verified by *Figure: 2*, where a 530 nm monomeric R6G absorption peak (S_0) with the vibronic shoulder at 490 nm were detected, this peak is attributed to $S_0\rightarrow S_1$ excitation. In addition, the spectrum also consists of three peaks at 347, 276, and 247 nm corresponding to the excited singlets S_2, S_3, and S_4, respectively which are in a good agreement with previous studies [28].

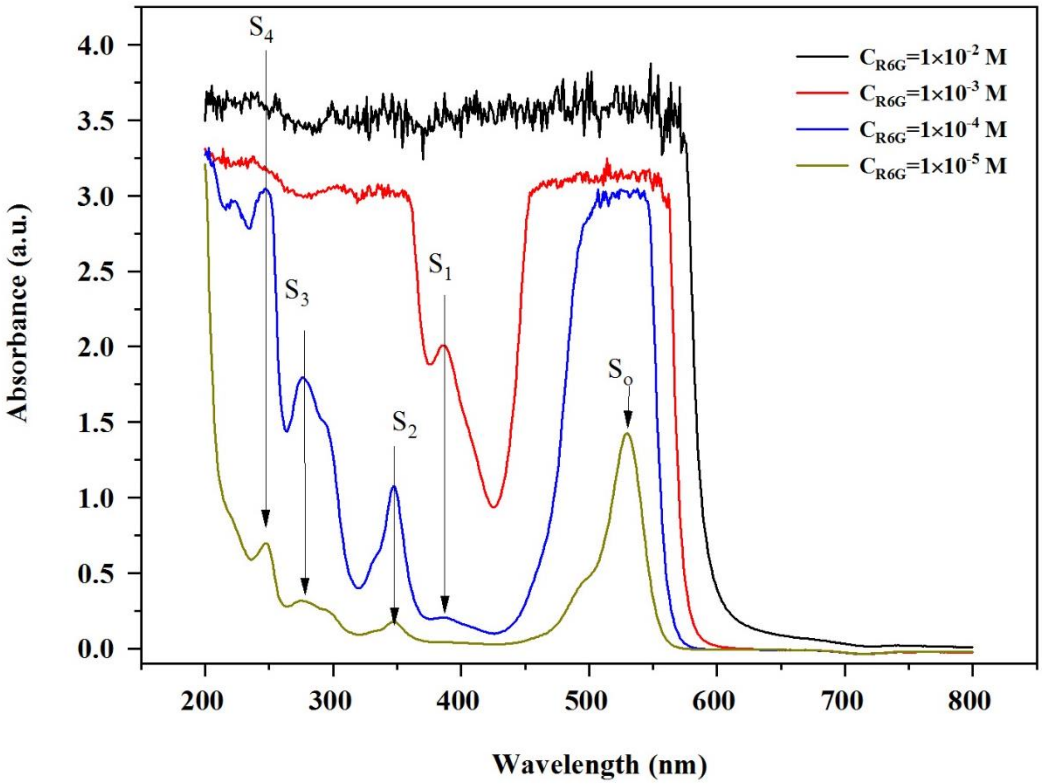

Figure-2: The Absorption spectra of R6G dye in EtOH solution at different molar concentrations.

Optical absorption spectra in UV-vis region of ageing pure and R6G doped TiO_2 sol with dye concentration ranging between 3×10^{-4} and 3×10^{-7} M, are given in *Figure: 3*. The sols were poured in a quartz cell of 1cm optical path. The pure sol spectrum shows a highly transparence in the visible region of (400-700) nm and there is a sharp rise in absorbance at the UV region. A strong absorbance in UV region as well as an absorption edge at 366 nm are detected, as shown in inset (a) of *Figure: 3*, which is due to the electronic transition from valance band to any point in the conduction band.

A red shift of the R6G doped TiO_2 sol absorption edge is observed by introducing the R6G dye with respect to the pure sol. From *Figure: 3*, a broad saturated band in the range of (460-560) nm for 3×10^{-4} M R6G is observed which is due to dye-dye interaction. While an absorption peak at 530 nm belong to $S_0\rightarrow S_1$ transition for all other concentration is observed; inset (b) shows this transition peak for 3×10^{-7} M concentration . The intensity of this peak increases with increasing dye concentration, which is consistent with Beer-Lambert law.

Figure: 4 shows the absorption spectra of the TiO_2 nanostructure coating thin films for pure and dye doped concentration in the range of (3×10^{-4}-3×10^{-7}) M on glass substrate. The spectra indicate a strong absorbance in the UV region, attributes to the TiO_2 electronic transition from valance band to the conduction band with a sharp rise of absorption edge a round 315 nm, as shown in inset (a) of *Figure: 4* and *Table:1*. The blue shift; about 50 nm, of the absorption edge for the TiO_2 coated thin films with respect to the sol ascribed to the quantum size effect, and this discrepancy proves the nanostructure texture of TiO_2 thin films [29].

In *Figure: 4*; inset (b), the absorption spectra for four concentration R6G doped TiO_2 thin films on glass substrate are shown. A broad absorption band centered at 401 nm in addition to a band around 490 nm of 3×10^{-4} M R6G are observed and it may refer to the formation dimeric dyes in the pores of the as-deposited amorphous TiO_2 coating films, where the films' matrix pores are filled with residual solvent. The dye concentration in the pores is higher than it in the sols [30].

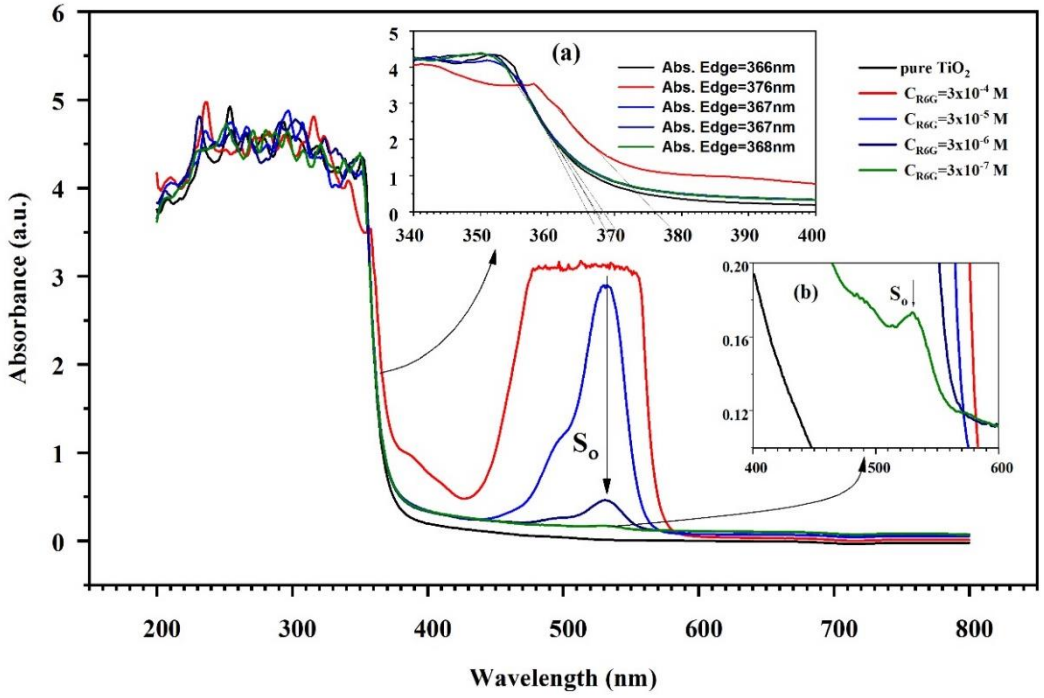

Figure-3: The absorption spectra of aged pure and R6G doped TiO_2 Sol at different molar concentrations. The inset; **(a)** shows absorption edge for all samples, **(b)** shows lowest concentration absorption peak (530 nm).

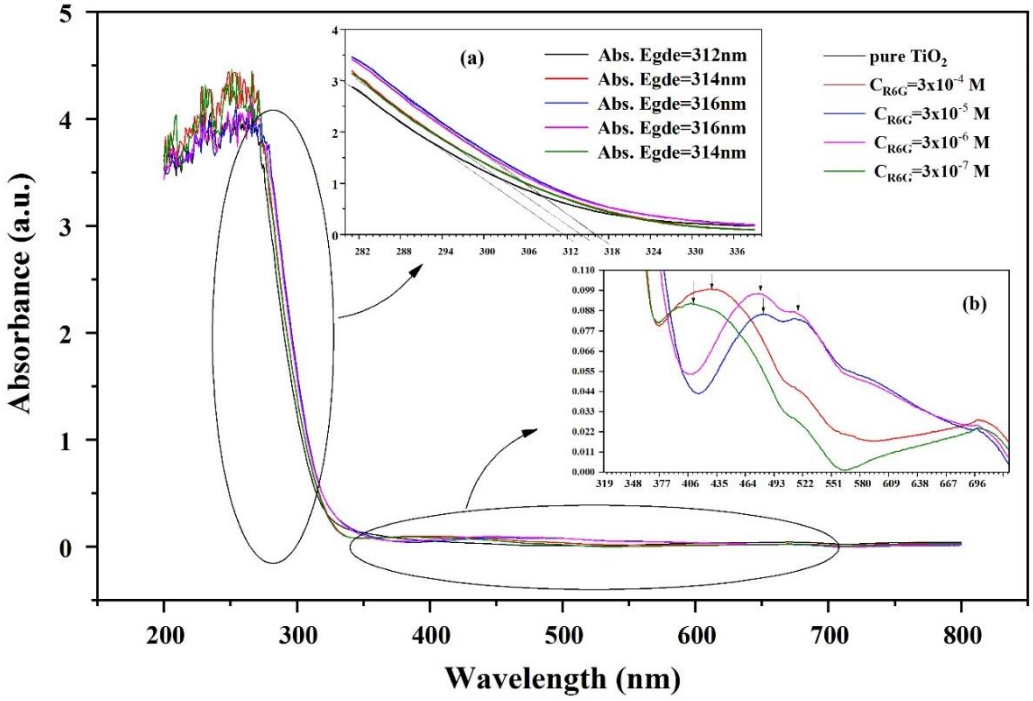

Figure-4: The absorption spectra of pure and different molar concentrations of R6G doped TiO_2 thin films on glass substrate. The inset; **(a)** shows absorption edge for all samples, **(b)** shows absorption peak of different C_{R6G}.

The peak to peak ratio of the dimeric absorption spectra (1: 0.44) indicates that the dye molecule-molecule interactions inside the matrix pores are more than the dye molecule-matrix surface interaction. For 3×10^{-5} M R6G, the dimer absorption spectrum consists of two separate bands at 454 and 483 nm with peak to peak ratio (0.86:0.84) which can be explained by the exciton theory. The exciton theory, a molecular quantum

mechanical theory based on monomer dipole-dipole interaction in the aggregates predicts a splitting of excited state changing the spectroscopy characteristics of the dimers [31].
As similar to 3×10^{-5} M, the absorption spectrum obtained from 3×10^{-6} M consists of two separate bands at 454 and 483 nm with peak to peak ratio (0.98:0.88), although it exhibits a red shift with respect to 3×10^{-5} M due to the dye aggregates formation which can affect the absorption spectrum characteristics by inducing the band splitting and spectral shifts, exciton theory.

Finally, a similar behavior for 3×10^{-7} M dye concentration is observed as 3×10^{-4} M which abroad band centered at 380 nm and a band nearly at 490 nm with peak to peak ratio (0.92:0.30) are noticed and may be attributed to the same reason of 3×10^{-4} M concentration.

Estimated Band Gap of Thin Films

The excitation of electrons from the valence band to conduction band of semiconductor metal oxide thin film perform, when the thin film absorbs photons of energy larger than the optical band gap which it is lead to a sharp increase in the absorbance of the semiconductor thin film to the wavelength corresponding to the optical band gap energy [32].

The UV-vis spectra of pure and different concentrations R6G doped TiO_2 sol and thin films onto glass substrate (as-deposited and dried at RT) are shown in Figures (3, 4); inset (a). The extrapolation straight line method was used to locate the absorption edge wavelength of the TiO_2 thin films, and the optical band gap of the samples were calculated from the equation E(eV)=1240/λ (nm), where λ is the wavelength of optical absorption edge in the absorbance spectrum [33]. The pure and doped TiO_2 thin film band gaps were estimated and listed in the *Table:1*.

The optical band gap for pure and doped TiO_2 coated thin films are approximately unchanged at 3.94 eV. This result is in agreement with the work of Valencia et al. 2010 [32]. This result may be belonged to the quantum size effect [29, 32].

Table-1: Absorption edge and band gap for pure and doped TiO_2 sol and thin films on glass substrate.

C_{R6G} (M)	Absorption Edge (nm)		Band Gap (eV)	
	Sol	Thin Film	Sol	Thin Films
0	366	312	3.39	3.97
3×10^{-4}	376	314	3.30	3.95
3×10^{-5}	367	316	3.38	3.92
3×10^{-6}	367	316	3.38	3.92
3×10^{-7}	378	314	3.28	3.95

Fluorescence Emission Spectra

A fluorescence is a spontaneous emission of radiation from the excited singlet states, in which the electron in the excited orbital has the opposite spin orientation as the ground-state electron. Also, the fluorescence emission spectra are a draw of the fluorescence intensity as a function of wavelength (nm) or wavenumber (cm^{-1}). It changes widely and depends upon many factors, some of them are; the fluorophore (dye) chemical structure and its solvent, pH of the environment, temperature, type and size of the host materials, as well as physical and chemical interactions of the dye with the host and other species [21, 25, 30]. Because fluorescence emission is caused by the recombination of free carriers, it may be used to disclose the effectiveness of charge carrier entrapment, immigration, and transfer, as well as to comprehend the fate of electron–hole pairs in semiconductor matrix [34].

The fluorescence spectra of R6G in EtOH solution with different concentration from 1×10^{-2} – 1×10^{-5} M were measured at RT and presented in *Figure: 5*. The dye solutions were tested in quartz cell of 1cm optical path. The maximum intensity wavelength of the fluorescence emission spectra was obviously found to be concentration dependent.

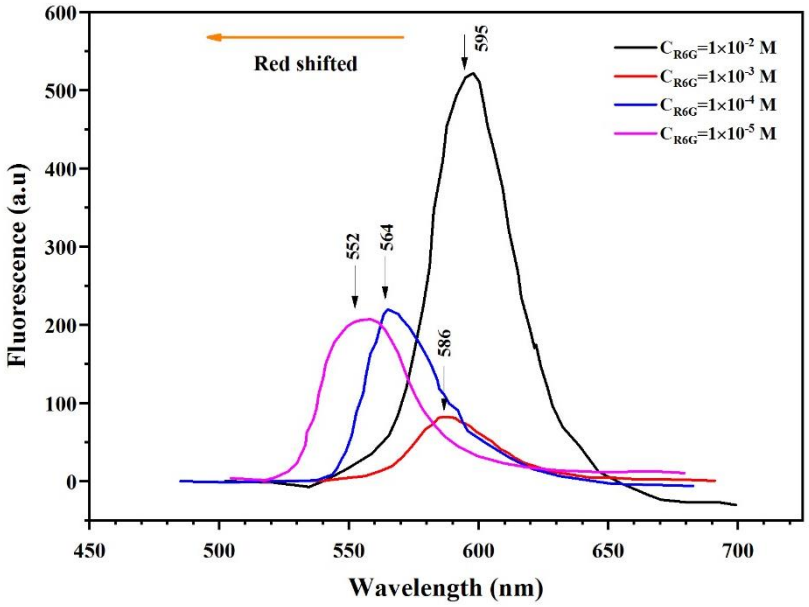

Figure-5: Fluorescence emission spectra of R6G dye in EtOH solution for different molar concentrations, at RT.

The maximum fluorescence emission wavelength is 552 nm for the dilute concentration of 1×10^{-5} M, and shifts to 595 nm with increasing the concentration into 1×10^{-2} M, as shown in *Table:2*. These values are in close agreement with the values reported by zehentbauer et al. [35]. In general, dyes dissolve in monomers, dimers, trimers, etc. At low concentration 1×10^{-5} M according to the absorption spectrum, monomers dominate. With increasing concentration, dimers and higher aggregates may gain importance. The red shift, suggesting that the fluorescent state of the dimers, trimers and higher aggregates are located at lower energies than the monomer excited state.

Table-2: Fluorescence Emission Peaks of 1×10^{-2} – 1×10^{-5} M R6G ethanolic solution.

C_{R6G} *(M)*	*Excitation Wavelength* λ_{exc} *(nm)*	*Emission Wavelength peaks* λ_{em} *(nm)*
1×10^{-2}	*514*	*595*
1×10^{-3}	*389, 504*	*586*
1×10^{-4}	*348, 522*	*564*
1×10^{-5}	*348, 530*	*552*

Figure: 6 presents normalized fluorescence spectra of R6G in TiO_2 sol at different concentration of the dye obtained at RT upon excitation the sols were tested in glass cell of 1cm optical path.
Similar to the absorption spectra, with increase of the dye concentration, the maximum emission spectra wavelength experienced a red shift as they are summarized in *Table:3*. The red shift is belonged to the dimerization of R6G molecules. For more explaining, the aggregation (e.g. dimerization), effect on colouristic photophysical properties of dye and therefore being of special characteristics. The dimerization formation may be led to absorption bond shifting, which in turn of affects the colour emission, that can be explained via

exciton theory by Kasha et al. ***[31]***. *Table 3* shows that the maximum emission wavelength is independent of the excited wavelength for all C_{R6G} doped TiO_2 sol. The results agree with kasha rule ***[31]***.

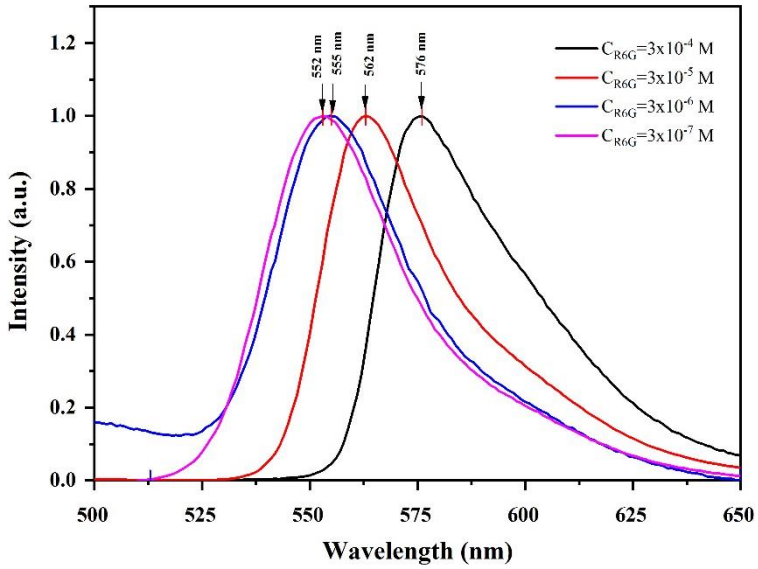

Figure 6: Fluorescence Emission spectra of R6G doped TiO_2 Sol for different molar concentrations, at RT.

Table-3: Fluorescence emission peaks of 3×10^{-4} – 3×10^{-7} M R6G doped TiO_2 Sol.

C_{R6G} *(M)*	***Excitation Wavelength*** λ_{exc} ***(nm)***	***Emission Wavelength*** λ_{em} ***(nm)***
3×10^{-7}	*340, 530*	*553*
3×10^{-6}	*340, 530*	*555*
3×10^{-5}	*340, 530*	*563*
3×10^{-4}	*340, 530*	*576*

The fluorescence spectra with 300 nm excitation wavelength of the different R6G dye concentration doped TiO_2 films; deposited on glass substrate, was measured. The fluorescence scan at the front-face (45º) films orientation; according to Bartl et.al. [26], was performed. There is a dramatic change in the fluorescence spectra upon changing from sol host to solid film host.

Typical fluorescence spectra of the dip-coated sol-gel R6G dye doped TiO_2 films on glass substrate at RT as a function of the C_{R6G} in the range of (3×10^{-4}-3×10^{-7}) M were presented in *Figure: 7*. Fluorescence scans were carried out between 310 and 700 nm using an excitation wavelength of 300 nm (~4 eV). For best appearance of fluorescence emission peaks and high intensity value, 4 eV excitation energy was chosen.

Figure: 7 shows different intensity peaks at (326, 347, 362, 378, 410, 475, and 486) nm belongs to TiO_2. The highest intensity of emission peak for all C_{R6G} is in ultraviolet UV band at 362 nm in addition to red band at 600 nm.

It is known that amorphous (a-TiO_2) is a semiconductor with a band gap of (~ 3.4-4.1) eV [36], and that UV light with wavelengths shorter than 330 nm (3.75 eV) can excite electrons above the band gap. The UV emission peak 326 nm corresponds to the band-to-band transition due to excitation of electrons from valence band to conduction band which agrees with the TiO_2 film's energy band gap result (~3.94 eV).

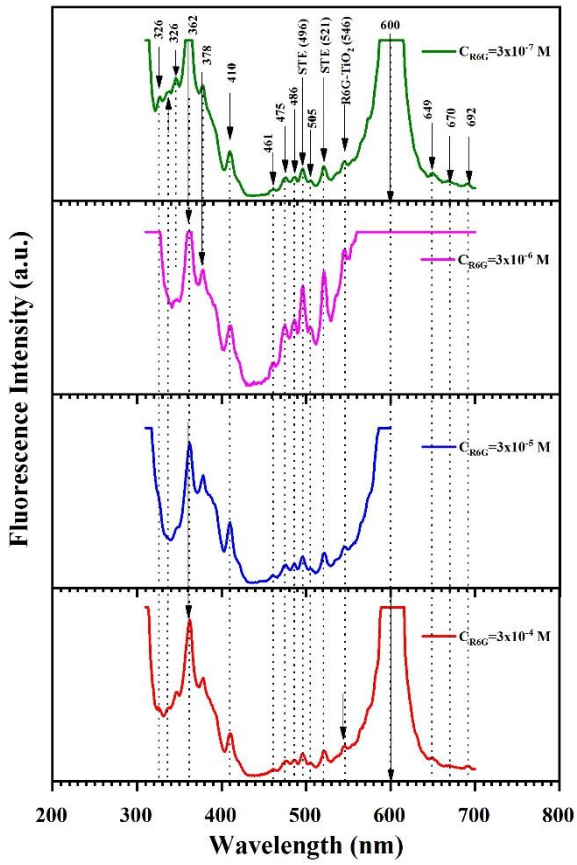

Figure 7: Fluorescence emission spectra of (Dip-Coated) sol-gel TiO_2 thin films doped with different C_{R6G} on glass with λ_{ex} =300 nm, at RT.

The shape and maximum fluorescence wavelength for all the films are almost the same because of the preparation condition were fixed through deposition process and the fluorescence spectra measurement. The difference in appearance might be due to the effect of different C_{R6G} (impurity) which effect on shallow and deep level emission throughout a profound influence on TiO_2 matrices structural defect.

The photoexcitation to conduction band leads to the self-trapping of the excitonic state, which causes strong self-trapped exciton (STE) emission at (362 nm), as shown in previous works [37, 38].

The self-trapped state is intrinsic exciton, an electronic excitation wave consisting of an electron-hole pair which propagates in a nonmetallic solid, that interacts with phonons, the lattice vibrations. The emission peaks have been interpreted as a recombination emission of a STE, which is formed, in turn, from a charge-transfer exciton. In TiO_2, STE seems to be insensitive to impurities and the probability of its formation in a TiO_6 octahedron depends on the strength of exciton-phonon coupling [37].

A well-defined emission peaks at 346, 378, and 410 nm are attributed to shallow trap center bellow the conduction band. From the bottom of conduction band few electrons jump to these shallow levels and then emit light at those above peaks [38]. Another peak at 475 and 486 nm with maximum intensity at 3×10^{-6} M of R6G concentration are observed in fluorescence spectrum, which belong to oxygen vacancy defect which including the electron transfer from Ti^{3+} to oxygen anion in a octahedral TiO_6^{8-} complex [34, 39]. Also, the 496 and 521 nm fluorescence peaks with the maximum intensity at the same above R6G concentration are noticed due to the emission of STE localized on titanate TiO_6 octahedra group in TiO_2 [40].

The existence of R6G dye molecules in TiO_2 film's matrix is a proved by showing up two different intensity peaks at 540 and 600 nm. The first weak peak, which is blue shifted with respect to its sol emission, is attributed to the interaction between the TiO_2 host matrix and R6G dye molecules [25], or with lower probability it may be due to TiO_2 matrix surface defects [38]. Whereas the second was very high intensity

emission at 600 nm, with shoulder at 573 nm, may belong to superposition between the molecular guest excited singlet states and TiO_2 defect states and hence an efficient energy transfers from these states to the R6G excited singlet states [3]. The above two peaks are in a good agreement with other articles [3, 25].

Finally, the trap levels at (649, 670, 692) nm are noticed only at minimum and maximum C_{R6G}. This interpreted that the R6G may decrease the Ti^{3+} defect since the electron trapped located at (0.7-1.6) eV bellow the conduction band edge contributes to the red band at wavelength around 590-700 nm [34, 39]. The fluorescence emission peaks of the dip-coated sol-gel R6G dye doped TiO_2 films on glass substrate were summarized in *Table:4.*

Table-4: Fluorescence emission peaks of 3×10^{-4} – 3×10^{-7} M R6G doped TiO_2 thin films on glass substrate with λ_{ex} =300nm.

Fluorescence Peaks Values (nm)				
$C_{R6G}=3\times10^{-4}$ M	***$C_{R6G}=3\times10^{-5}$ M***	***$C_{R6G}=3\times10^{-6}$ M***	***$C_{R6G}=3\times10^{-7}$ M***	***Peak's Energy (eV)***
326			*327*	*3.80*
337			*337*	*3.68*
347		*347*	*346*	*3.57*
362	*362*	*362*	*362*	*3.43*
378	*378*	*378*	*378*	*3.28*
410	*410*	*409*	*410*	*3.02*
461	*461*	*462*	*461*	*2.69*
475	*476*	*475*	*476*	*2.61*
486	*486*	*486*	*486*	*2.55*
496	*496*	*496*	*496*	*2.50*
505	*505*	*505*	*505*	*2.46*
521	*522*	*521*	*521*	*2.38*
546	*545*	*546*	*546*	*2.27*
600(573 shoulder)			*600(573 shoulder)*	*2.07*
649				*1.91*
670				*1.85*
692				*1.79*

Conclusions

In this paper, dip-coating technique via low temperature wet chemical sol–gel process, was effectively used to synthesize pure and R6G doped TiO_2 nanostructured thin films on glass substrate. The prepared thin films were analyzed using XRD, and the patterns did not show any evidence peak related to TiO_2 phase which indicate that doped and undoped TiO_2 matrices are primarily amorphous. Absorption spectra of R6G solution, sol, and thin films were recorded. A 530 nm monomeric absorption peak with the vibronic shoulder at 490 nm of low concentration R6G ethanolic solution were detected which indicates that R6G dye dissolves completely into monomer. Absorption edge of the R6G doped TiO_2 sol was experience to a small red shift with respect to the pure sol. Absorption peak at 530 nm for all doped sols was observed. The absorption spectra for all pure and doped TiO_2 films indicate a strong absorbance in the UV region and 50 nm blue shift of the absorption edge with respect to the sol that proves the nanostructure texture of TiO_2 thin films. The dye aggregates formation in the pores of the as-deposited amorphous doped TiO_2 coated films change the absorption spectrum features by inducing band splitting and spectral shifts, which may be explained by the exciton theory.

Maximum fluorescence emission peak of R6G ethanolic solution and doped TiO_2 sol exhibit a red shift with increasing of the dye concentration. The existence of R6G dye molecules in TiO_2 film's matrix is a proved by showing up two different intensity fluorescence peaks at 540 and 600 nm. So the manufacturing the hybrid R6G-TiO_2 active medium laser and optoelectronic device can be suggested.

References

[1] Xia, Y., Yang, P., Sun, Y., Wu, Y., Mayers, B., Gates, B., Yin, Y., Kim, F. and Yan, H. *"One-Dimensional Nanostructures: Synthesis, Characterization, and Applications"*, Advanced Materials, Vol. (15), Issue. 5, pp.353-389. (2003).

[2] Reisfeld, R. *"Prospects of sol–gel technology towards luminescent materials"*, Optical Materials, Vol. (16), pp.1-7. (2001).

[3] de Azevedo, W. M., da Silva Jr, E. F., Pepe, I., Ferreira da Silva, A., Tomas, S. A., Palomino, R., Lozada, R., Persson, C., and Ahuja, R. *"Spectroscopic Properties of TiO_2 Sol-Gel Films Doped with Rhodamine 6G Dye"*, 3rd Brazil MRS Meeting, Symposium A, October 10-13, (2004).

[4] Ameen, M. A. and Arif, G. K. *"Structural and spectroscopic study of Ho^{3+}-doped nanotitania host prepared using a sol–gel technique". Luminescence*, Vol. (35), pp. 1109– 1117 (2020).

[5] Gupta, K.K., Jassal, M. and Agrawal, A.K. *"Sol-gel derived titanium dioxide finishing of cotton fabric for self cleaning"*, Indian Journal of Fibre and Textile Research, Vol. (33), pp. 443–450 (2008).

[6] Zarzycki, J., Prassas, M. and Phalippou, J. *" Synthesis of glasses from gels: the problem of monolithic gels"*, Journal of Materials Science, Vol. (17), pp. 3371–3379 (1982).

[7] Brinker, C. J. and Scherer, G. W. *"Sol-Gel Science: the Physics and Chemistry of Sol-Gel Processing"*, San Diego, Academic Press, Inc., (1990).

[8] Dislich, H. *"Sol-Gel Technology for Thin Films, Fibers, Preforms, Electronics, and Specialty Shapes"*, Ed. L. C. Klein, New Jersey, Noyes Publications, pp. 50. (1988).

[9] Livage, J., Babonneau, F. and Sanchez, C. *"sol-gel chemistry for optical material, in Sol-Gel Optics Processing and Applications"*, Ed. L. C. Klein, New York, Springer Science and Business Media, LLC, pp. 39. (1994).

[10] Palomino-Merino, R., Torres-Kauffman, J., Lozada-Morales, R., Portillo-Moreno, O., Garcia-Rocha, M. and Zelaya-Angel, O. *"Photoluminescence of Rhodamine 6G-doped amorphous TiO_2 thin films grown by sol–gel"*, Vacuum, Vol. (81), pp. 1480–1483 (2007).

[11] Nahak, B. K., Subudhi, T. S. K., Pradhan, L. K., Panigrahi, A., Roshan, R., Mahato, S. S. and Mahata, S. *" An Investigation on Photocatalytic Dye Degradation of Rhodamine 6G Dye with Fe- and Ag-Doped TiO2 Thin Films"*, Proceedings of the Fourth International Conference on Microelectronics, Computing and Communication Systems (MCCS 2019), pp. 295-307 (2019).

[12] Chrysicopoulou, P., Davazoglou, D., Trapalis, Chr. and Kordas G. *"Optical properties of very thin (<100 nm) sol–gel TiO_2 films"*, Thin Solid Films, Vol. (323), pp. 188–193 (1998).

[13] Su, C., Hong, B.-Y. and Tseng, C.-M. *"Sol–gel preparation and photocatalysis of titanium dioxide"*, Catalysis Today, Vol. (96), pp. 119–126 (2004).

[14] Lange, R. W. and Sowman, H. G. "Shaped and Fired Articles of TiO_2". U.S. Pat. No. 4 166 147, (1979).

[15] Burns, A., Hayes, G., Li, W., Hirvonen, J., Demaree, J. D. and Shah, S. I. *"Neodymium ion dopant effects on the phase transformation in sol–gel derived titania nanostructures"*, Materials Science and Engineering: B, Vol. (111), Issues 2–3, pp. 150-155 (2004).

[16] Sanchez C. and Ribot, F. *"Design of hybrid organic-inorganic materials synthesized via sol-gel chemistry"*, New Journal of Chemistry, Vol. (18), pp. 1007-1047 (1994).

[17] Tomas, S. A., Stolik, S., Palomino, R., Lozada, R., Persson, C., Ahuja, R., Pepe, I. and da Silva, A. F. *"Optical properties of rhodamine 6G-doped TiO2 sol-gel films"*, Journal de Physique IV France, Vol. (125), pp. 415-417 (2005).

[18] Wang, X., Wu, G., Zhou, B. and Shen, J. *"Optical Constants of Crystallized TiO_2 Coatings Prepared by Sol-Gel Process"*, Materials, Vol. (6), pp. 2819-2830 (2013).

[19] Park, Y. R. and Kim, K. J. *"Structural and optical properties of rutile and anatase TiO_2 thin films: Effects of Co doping"*, Thin Solid Films, Vol. (484), pp. 34– 38 (2005).

[20] Reisfeld, R., Brusilovsky, D., Eyal, M., Miron, E., Burstein, Z. and Ivri, J. *"A new solid-state tunable laser in the visible"*, Chemical Physics Letters, Vol. (160), No. 1, pp. 43-44 (1989).

[21] Arbeloa, F. L., Gonzalez, I. L., Ojeda, P. R. and Arbeloa, I. L. *"Aggregate Formation of Rhodamine 6G in Aqueous Solution"*, Journal of the Chemical Society, Faraday Transactions 2, Vol. (78), pp. 989-994 (1982).

[22] On, C., Tanyi, E. K., Harrison, E., and Noginov, M. A. *"Effect of molecular concentration on spectroscopic properties of poly(methylmethacrylate) thin films doped with rhodamine 6G dye"*, Optical Materials Express, Vol. (7), No. 12, pp. 4286-4295 (2017).

[23] Jensen, L. and Schatz, G. C. *"Resonance Raman Scattering of Rhodamine 6G as Calculated Using Time-Dependent Density Functional Theory"*, Journal of Physical Chemistry A, Vol. (110), No. 18, pp. 5973-5977 (2006).

[24] Sugiarto, I. T., Isnaeni and Putri, K. Y. *"Analysis of dual peak emission from Rhodamine 6G organic dyes using photoluminescence"*, Journal of Physics: Conference Series, Vol. (817), pp. 012047-1-012047-6 (2017).

[25] Vogel, R., Meredith, P., Harvey, M.D. and Rubinsztein-Dunlop, H. *"Absorption and fluorescence spectroscopy of rhodamine 6G in titanium dioxide nanocomposites"*, Spectrochimica Acta Part A, Vol. (60), pp. 245–249 (2004).

[26] Bartl, M. H., Boettcher, S. W., Hu, E. L., and Stucky, G. D. *"Dye-activated hybrid organic/inorganic mesostructured titania waveguides"*, Journal of American Chemical Society, Vol. (126), pp. 10826-10827 (2004).

[27] Grabis, J., Karashanova, D., Filkova, D., Garlanov, D. and Vissokov, G. *"Synthesis and Characterization of Nanosized Composite Material Consisting of Ferromagnetic Core and Insulating Shell, in Nanoscience & Nanotechnology, Issue 12"*, Eds. Balabanova, E. and Mileva, E., Bulgaria, BAS and NCCNT, pp. 19-22 (2012).

[28] Venkateswarlu, P., George, M. C., Rao, Y. V., Jagannath, H., Chakrapani, G. and Miahnahri, A. *"Transient excited singlet state absorption in Rhodamine 6G"*, Pramana - J Phys, Vol. (28), No. 1, pp. 59–71 (1987).

[29] Chen, X. and Mao, S.S. *"Titanium Dioxide Nanomaterials: Synthesis, Properties, Modifications, and Applications"*, Chemical Reviews, Vol. (107), No. 7, pp. 2891–2959 (2007).

[30] Innocenzi, P., Kozuka, H. and Yoko, T. *"Dimer-to-monomer transformation of rhodamine 6G in sol—gel silica films"*, Journal of Non-Crystalline Solids, Vol. (201), pp. 26-36 (1996).

[31] Kasha, M., Rawls, H. R. and Ashraf El-Bayoumi, M. "*The exciton model in molecular spectroscopy*", Pure and Applied Chemistry, Vol. (11), No. 3-4, pp. 371-392 (1965).

[32] Valencia, S., Marín, J. M. and Restrepo, G. "*Study of the Bandgap of Synthesized Titanium Dioxide Nanoparticules Using the Sol-Gel Method and a Hydrothermal Treatment*", The Open Materials Science Journal, Vol. (4), pp. 9-14 (2009).

[33] Gonçalves, M. C., Pereira, J. C., Matos, J. C. and Vasconcelos, H. C. *"Photonic Band Gap and Bactericide Performance of Amorphous Sol-Gel Titania: An Alternative to Crystalline TiO_2 "*, Molecules, Vol. (23), pp. 1677–1696 (2018).

[34] Li, F.B. and Li, X.Z. *"The enhancement of photodegradation efficiency using Pt–TiO_2 catalyst"*, Chemosphere, Vol. (48), pp. 1103–1111 (2002).

[35] Zehentbauer, F.M., Moretto, C., Stephen, R., Thevar, T., Gilchrist, J.R., Pokrajac, D., Richard, K.L. and Kiefer, J. *"Fluorescence spectroscopy of Rhodamine 6G: Concentration and solvent effects"*, Spectrochimica Acta Part A: Molecular and Biomolecular Spectroscopy, Vol. (121), pp. 147–151 (2014).

[36] Gao, Y., Masuda, Y., Peng, Z., Yonezawa, T. and Koumoto, K. *"Room temperature deposition of a TiO_2 thin film from aqueous peroxotitanate solution"*, Journal of Materials Chemistry, Vol. (13), pp. 608–613 (2003).

[37] Sildos, I., Suisalu, A., Aarik, T., Sekiya, J. and Kurita, S. "*Self-trapped exciton emission in crystalline anatase*", Journal of Luminescence, Vol. (87-89), pp. 290-292 (2009).

[38] Abdullah, S. A., Sahdan, M. Z., Nafarizal, N., Saim, H., Bakri, A. S., Cik Rohaida, C. H., Adriyanto, F. and Sari, Y. *"Photoluminescence study of trap-state defect on TiO_2 thin films at different substrate temperature via RF magnetron sputtering"*, Journal of Physics: Conference Series, Vol. (995), pp. 012067-1-012067-9 (2018).

[39] Yu, J. C., Yu, J., Ho, W., Jiang, Z. and Zhang, L. *"Effects of F- Doping on the Photocatalytic Activity and Microstructures of Nanocrystalline TiO_2 Powders"*, Chemistry of Materials, Vol. (14), pp. 3808-3816 (2002).

[40] Deb, S. K. *"Photoconductivity and photoluminescence in amorphous titanium dioxide"*, Solid State Communications, Vol. (11), pp. 713-715 (1972).